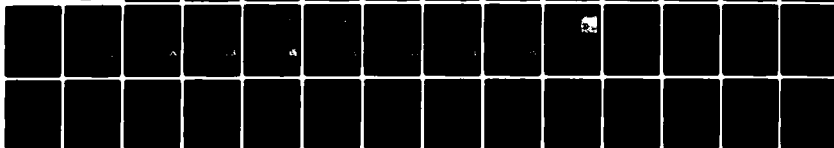


AD-A111 435

SOUTHEASTERN MASSACHUSETTS UNIV NORTH DARTMOUTH DEPT —ETC F/8 9/2
A FURTHER STUDY OF THE MULTICHANNEL MAXIMUM ENTROPY SPECTRAL AN—ETC(U)
FEB 82 C H CHEN; G YOUNG N00014-79-C-0494
SMU-ZE-TR-82-03 NL

UNCLASSIFIED

101
0525



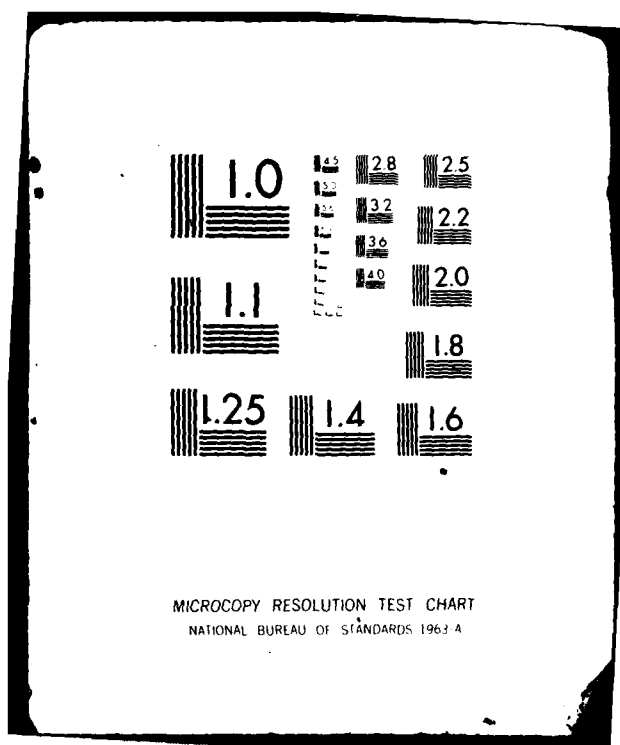
END

DATE

FILED

9-82

DTIC



Technical Report
DPO-EM-TR-82-03
Contract Number N00014-79-C-0494
February 19, 1982

①

ADA111435

A Further Study of the
Multichannel Maximum
Entropy Spectral Analysis*

DTIC
ELECTE
MAR 1 1982

by
C. H. Chen
Gia-kun Young
Department of Electrical Engineering
Northeastern Massachusetts University
North Dartmouth, Massachusetts 02747

DTIC FILE COPY

*The support of the Statistics and Probability Program of the Office of Naval Research on this work is gratefully acknowledged.

DISTRIBUTION STATEMENT A

Approved for public release;
Distribution Unlimited

82 00 005

A Further Study of the Multichannel Maximum Entropy Spectral Analysis

1. Introduction

In the field of signal detection and estimation, it is always necessary to face the problems with systems whose states are described by several time variables. For example, in the geophysical research, data are gathered by arrays of sensors (seismographs, hydrophones, antennas, meteorological stations). The sensors used in these array systems will not always be along a line or in a regular grid but will often have some arbitrary spatial distribution. Also, in an array system, one or more sensors can be connected to a channel; each of these channels provides one of the signal to be processed. Instead of processing the signals received on each channel separately, it is possible to process all the received signals collectively by means of a multichannel filter that takes into account the interrelations among the individual signals. Therefore, multichannel time series processing is quite important because of its sufficient informations about the object. To solve this problem, spectral estimation is an effective tool to describe the signal properties. Various attempts [1] - [4], [8] - [9] of multichannel spectral analysis have been made in the literature. Many conventional methods have been extended from one channel to multichannel. One technique which has been studied extensively due to its high resolution characteristics is the maximum entropy method (MEM). Jones [3], Nuttall [4], Strand [1] and Morf et al. [2] have independently obtained the multichannel generalization of the scalar Burg's maximum entropy method. In this report, we use the generalization method of Strand

as a means of study. Detailed computer results are presented for the multichannel maximum entropy spectral analysis of short sinusoids. Although for the real signals the spectral line shifting and spontaneous line splitting are observed, we have demonstrated that such phenomena are almost completely eliminated in the complex signal case. This result is practically significant as it indicates that accurate spectral estimation is possible for the complex signal case. The multichannel maximum entropy spectral analysis can thus provide a good phase estimate from which time delays among spatially separated sensors can be properly determined.

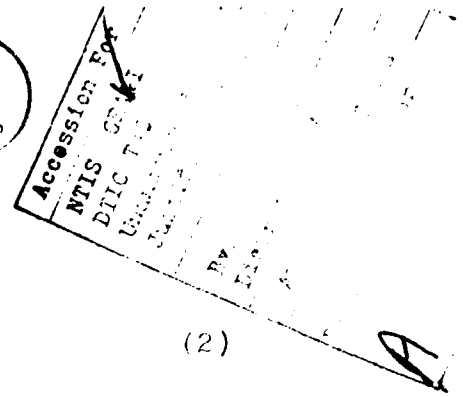
This report is organized as follows. In section II, we briefly review the algorithm of Strand. In section III, we show the results of the spectral estimation and the phase difference between channels. In section IV, we present the comparative result of the real signals and the complex signals in the viewpoint of line shifting and splitting properties. And in the Appendix, we list a detailed computer program in Fortran which we used to obtain the complex multichannel maximum entropy spectral estimation.

II. Theoretical Background

Let

$$y(t) = \begin{bmatrix} y_1(t) \\ y_2(t) \\ \vdots \\ y_p(t) \end{bmatrix}, \quad t = \{ n \Delta t \}_{n=-\infty}^{\infty} \quad (1)$$

be a complex zero-mean, wide-sense stationary p-channel time series. The N-element forward filter (or forward filter of length N)



has the form.

$$y(t) + \sum_{k=1}^N F_{kN}^* y(t-k\Delta t) = e_N(t) \quad (2)$$

Similarly, we consider the N-element backward filter

$$y(t) + \sum_{k=1}^N B_{kN}^* y(t+k\Delta t) = b_N(t) \quad (3)$$

In (2) and (3), the forward and backward filter coefficients, F_{kN} and B_{kN} , respectively, are complex $p \times p$ matrices. The asterisk * denotes the (Hermitian) conjugate transpose. For the optimum forward or backward filters (2) or (3), we impose the condition that the expected mean-square value of $e_N(t)$ or $b_N(t)$ should be a minimum. For (2) this involves determining $F_{1N}, F_{2N}, \dots, F_{NN}$ such that

$$E \left\{ \left[e_N(t) \right]^* \left[e_N(t) \right] \right\} = \text{minimum} \quad (4)$$

where $E \{ \quad \}$ denotes the expected value. Inserting (2) into (4) and minimizing with respect to the coefficients F_{kN}^* gives the system

$$\begin{bmatrix} R_0 & R_1 & R_2 & \dots & R_N \\ R_{-1} & R_0 & R_1 & \dots & R_{N-1} \\ \vdots & \vdots & \vdots & & \vdots \\ R_{-N} & R_{-N+1} & R_{-N+2} & & R_0 \end{bmatrix} \begin{bmatrix} I \\ F_{1N} \\ \vdots \\ F_{NN} \end{bmatrix} = \begin{bmatrix} P_N \\ 0 \\ \vdots \\ 0 \end{bmatrix} \quad (5)$$

where I is the $p \times p$ identity matrix and the square block submatrices in this system are defined by

$$R_k = E \left\{ y(t) y^*(t - k\Delta t) \right\}, \quad k=0, 1, \dots, N \quad (6)$$

so that

$$R_{-k} = R_k^* \quad (7)$$

We call the coefficient matrix in (5) the R-matrix, or simply R. The forward power matrix P_N for the resulting optimum filter (that is, for F_{kN} satisfying (5)) is

$$P_N = E \left\{ e_N(t) e_N^*(t) \right\} \quad (8)$$

By multiplying both sides of (5) by F_N^* we have,

$$P_N = F_N^* R F_N \quad (9)$$

where we define F_N by

$$F_N^* = \left[I, F_{1N}^*, \dots, F_{NN}^* \right]$$

with comma indicating matrix partition.

Similarly, for the optimum backward filter, we can derive a system:

$$\begin{bmatrix} R_0 & R_{-1} & R_{-2} \dots & R_{-N} \\ R_1 & R_0 & R_{-1} \dots & R_{-N+1} \\ \vdots & \vdots & \vdots & \vdots \\ R_N & R_{N-1} & R_{N-2} \dots & R_0 \end{bmatrix} \begin{bmatrix} I \\ E_{1N} \\ \vdots \\ B_{NN} \end{bmatrix} = \begin{bmatrix} P_N^* \\ 0 \\ \vdots \\ 0 \end{bmatrix} \quad (10)$$

We call the coefficient matrix in (10) the R' matrix, or simply R' .

The backward power matrix P_N' for the resulting optimum filter is

$$P_N' = E \left\{ b_N(t) b_N^*(t) \right\} \quad (11)$$

and it follows from (10) that

$$P_N' = B_N^* R' B_N \quad (12)$$

where

$$B_N^* = \left[I, B_{1N}^*, \dots, B_{NN}^* \right]$$

Purg has derived the following results concerning the recursive solution of (5) and (10), the forward and backward filters may be postulated in the form

$$F_N = \begin{bmatrix} F_{N-1} \\ 0 \end{bmatrix} + \begin{bmatrix} 0 \\ b_{N-1}' \end{bmatrix} C_N \quad \text{and} \quad B_N = \begin{bmatrix} F_{N-1} \\ 0 \end{bmatrix} C_N' + \begin{bmatrix} 0 \\ b_{N-1}' \end{bmatrix} \quad (13)$$

where $B_{N-1}' = [B_{N-1,N-1}^* \dots B_{N-1,1}^*]^*$ is the block reverse of B_{N-1} , and the p x p matrices C_N and C_N' are called forward and backward reflection coefficients, respectively. It can be shown that P_N and P_N' may be computed by using the modern Levinson algorithm:

$$P_N = P_{N-1} - C_{N-1}^* P_{N-1}' C_{N-1} \quad (14)$$

$$P_N' = P_{N-1}' - (C_{N-1}')^* P_{N-1} C_{N-1}' \quad (15)$$

and

$$C_N = (P_{N-1}')^{-1} (C_{N-1}')^* P_{N-1}$$

and

$$C_N' = (P_{N-1})^{-1} C_{N-1}^* P_{N-1}' \quad (16)$$

For the positive definite $P_N > 0$ (and $P_N' > 0$), it is known that the maximum entropy (autoregressive) power spectral density, $S(f)$, a p x p matrix, can then be calculated from the forward filter F_N by

$$S(f) = \Delta t \left[F^{-1}\left(\frac{1}{z}\right) \right]^* P_N \left[F^{-1}\left(\frac{1}{z}\right) \right] \quad (17)$$

where $F(z) = 1 + F_{10}z + \dots + F_{N0}z^N$, z is the complex scalar defined by $z = \exp \left[-2\pi i f \Delta t \right]$ and f is the frequency.

It can be shown (as suggested in (9)) that P_0, P_1, \dots, P_N and $(P_0', P_1', \dots, P_N')$ are positive definite if and only if R is positive definite. Instead of trying to solve (5) using approximations to the R_k , Strand [1] derived a method of estimating the reflection coefficients

C_N and C'_N by minimizing a certain weighted sum of squares of residuals for the forward and backward filters, after which all forward and backward filter coefficients $F_{k,l}$ and $B_{k,l}$ are obtained by the modern Levinson algorithm. It can be shown that

$$B C_N + P'_{N-1} C'_N P'_{N-1} E = -2G \quad (18)$$

where

$$\begin{aligned} E &= \sum_{m=1}^M \bar{W}_m e_m^N (e_m^N)^* \\ G &= \sum_{m=1}^M \bar{W}_m b_m^N (e_m^N)^* \\ B &= \sum_{m=1}^M \bar{W}_m b_m^N (b_m^N)^* \end{aligned} \quad (19)$$

and \bar{W}_m are positive scalar weights (usually all taken as $\frac{1}{N}$ in practice). Nd is the number of observation of a realization of $y(t)$, N is the number of tuples of data.

Also e_m^N and b_m^N can be obtained from

$$e_m^N = e_m^{N-1} + C_{N-1}^* b_{m+1}^{N-1}$$

and

$$b_m^N = b_m^{N-1} + (C_{N-1}')^* e_m^{N-1} \quad (20)$$

$$m=1, 2, \dots, Nd-N = M, N > 1$$

The whole computing procedure is illustrated in Fig. 1.

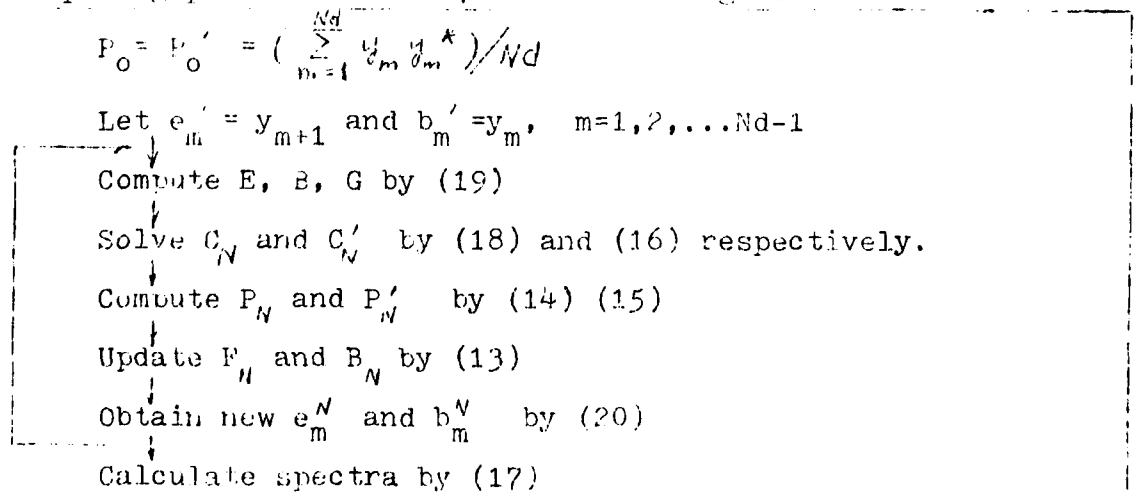


Fig. 1 Computing procedure for the multichannel Maximum Entropy process

111. Numerical Results of the Multichannel MFM Spectrum and Estimation of Phase Differences Between Channels

To ensure the correctness of the program, the same data which Strand used have been tested:

N_d (number of data points sampled) = 128

Δt = 1 second.

p (number of channels) = 2

$$y_t = \begin{bmatrix} y_{1t} \\ y_{2t} \end{bmatrix}, \quad t=1,2,\dots, 128$$

$$\text{Re } y_{1t} = \cos(2\pi f_1 t + \phi_1) + 0.25(\text{Ranf} - 0.5)$$

$$\text{Im } y_{1t} = \sin(2\pi f_1 t + \phi_1) + 0.25(\text{Ranf} - 0.5) \quad (21)$$

$$\text{Re } y_{2t} = \cos(2\pi f_2 t + \phi_2) + 0.25(\text{Ranf} - 0.5)$$

$$\text{Im } y_{2t} = \sin(2\pi f_2 t + \phi_2) + 0.25(\text{Ranf} - 0.5)$$

where Ranf is a pseudo-random number uniformly distributed between 0 and 1, ϕ_d is the phase difference between channels and f_i is the input frequency. If we denote the spectrum by

$$S(f) = \begin{bmatrix} S_{11}(f) & S_{12}(f) \\ S_{21}(f) & S_{22}(f) \end{bmatrix} \quad (22)$$

where f is the frequency in Hz, then the squared coherence is given by

$$\text{coh}^2(f) = \frac{|S_{12}(f)|^2}{S_{11}(f) S_{22}(f)} \quad (23)$$

A rough indication of the expected performance is given by Akaike's FPE criterion, given by

$$\text{FPE}(N) = \det P_n \left(\frac{N_d + 1 + pN}{N_d - 1 - pN} \right)^p$$

Figs. 2a and 2b show $S_{11}(f)$ and $S_{22}(f)$ for the real sinusoid inputs with $f = 0.0625$ Hz, $\psi_d = 1$ rad. and NPEF (number of terms in the prediction error filter) = 7. The results for $S_{12}(f)$ are shown (in amplitude and phase) in Figs. 2c and 2d. From Fig. 2d, we can observe that the phase of $S_{12}(f)$ appears to equal -1 radian at $f = 0.0625$ Hz. In Fig. 2e, the squared coherence is shown. Fig. 2f and Fig. 2g also indicate the maximum and minimum eigenvalues of spectra. Figs. 3a-3g is the repeated procedure of Figs. 2a-2g but with complex input signals. The comparison shows that the complex multichannel MEM gives better resolution and accuracy than the real case.

It is well known that the phase difference between channels is a very important parameter. Correct phase difference can give very good estimation of time delay so as to detect the location of the target. Different sets of data have been tested using the complex multichannel MEM program with phase difference $\psi_d = 0.5$ rad, -1 rad, 2 rad. ($f_1 = 0.0625$ Hz), $\psi_d = -0.5$ rad ($f_1 = 0.2$ Hz). The results of 1-1 spectrum $S_{11}(f)$ and phase of 1-2 spectrum, $\arg. S_{12}(f)$ are shown in Figs. 4(a,b), 5(a,b), 6(a,b) and 7(a,b) respectively.

It is noted that the results are satisfactory.

IV. The Splitting and Shifting Problem in Multichannel MEM Power Spectra

In 1974, Chen and Stegen [7] ran some computer experiments. They noted that the estimated spectral maximum was found to shift in relation to the true maximum. The frequency shifts depended upon the initial phase and the length of the sinusoid. Fougere et al. [6] showed that the problem arose from the assumption of Burg that

previously determined reflection coefficient are held fixed in order to determine the present reflection coefficients. Also, Bougere [5] recently indicated that these properties occurred to the single channel complex signals and the multichannel real signals. In order to study this problem we have tested a signal which exemplified the problem for the single-channel signals but in both real and complex cases. This is a single sine wave of frequency 1 Hz sampled every 0.05 seconds, with additive noise:

$$\text{Re } f_1(n) = \cos((n-1)\pi/10 + \phi_1) + Ag_1(n)$$

$$\text{Im } f_1(n) = \sin((n-1)\pi/10 + \phi_1) + Ag_1(n)$$

$$\text{Re } f_2(n) = \cos((n-1)\pi/10 + \phi_2) + Ag_2(n)$$

$$\text{Im } f_2(n) = \sin((n-1)\pi/10 + \phi_2) + Ag_2(n)$$

where ϕ_1 and ϕ_2 are initial phases in each channel and $g_1(n)$ and $g_2(n)$ are independent realizations of random numbers in the range ± 0.5 and A is the noise amplitude. Also, we used Nd and $NPEF$ to represent the number of data points and the number of terms in the prediction error filter respectively.

We have noted that the number of terms of filter ($NPEF$) affect the quality of the spectrum as indicated by Fig. 8a with $NPEF=3,9,21$. The same data are applied to the real and complex multichannel cases as shown in Fig. 8b, 8c respectively. We can see the real multichannel case is worse even than the single channel case (for $NPEF=21$), but the complex signal performs good. Figs. 9-11 show the effects of the number of data sample (Nd) to the location of spectral peak of real signals. Figs. 9a, 10a, 11a show the location of spectral peak is farther from 1 Hz as the cycles are not

completed. When the number of data points increases, the frequency shift decreases as shown in Fig. 14. As expected there is a node at $N_d=21, 41, \dots$, every full cycle, where there is excellent agreement between true and apparent frequencies. However, Figs. 12a, 13a show two more cases but with different initial phase angles. The locations of spectral peak for various number of data are also shown in Figs. 15 and 16 respectively (for $\psi_1=45^\circ$, $\psi_2=135^\circ$ and $\psi_1=-45^\circ$,

$\psi_2=-135^\circ$). Again we have noted the same property which is affected by the number of data points sampled. Comparing the location of the peak of $N_d=21$ of Figs. 9a, 12a and 13a, and the vertical axis of Figs. 14, 15, and 16, we have noted the peak of the real multichannel case is also affected by the initial phase. The peak with $45^\circ, 135^\circ$ phases shifts farther than with $0^\circ, 180^\circ$ case. This is the same condition as in the single channel case.

A very interesting property is that the location of spectral peaks does not shift away from the true value for various variations (number of data sampled, number of terms in the prediction error filter, value of initial phase). From Figs. 9b-13b and Figs. 14-16, the complex multichannel case always gives very satisfactory results. Therefore, we can conclude that the complex MEM power spectrum estimation is not affected by the factors indicated above because of its sufficient informations.

References

1. O. N. Strand, "Multichannel complex maximum entropy (autoregressive) spectral analysis," IEEE Trans. Automat. Contr., vol. AC-22, no. 4, pp. 634-640, August 1977.
2. M. Norf, A. Vieira, D. T. L. Lee and T. Eulath, "Recursive multichannel maximum entropy spectral estimation," IEEE Trans. on Geoscience Electronics, vol. GE-16, no. 2, pp. 88-94, April 1978.
3. R. H. Jones, "Multivariate autoregression estimation using residuals," in Applied Time Series Analysis edited by N. F. Findley, Academic Press, 1978.
4. A. S. Nutall, "Fortran program for multivariate linear predictive spectral analysis, employing forward and backward averaging," NUCS Technical Document 5419, Naval Underwater Systems Center, New London, Conn. 1976.
5. L. F. Fougere, "Spontaneous line splitting in multichannel maximum entropy power spectra," proceedings of the 1st AGSI Workshop on Spectral Estimation, Hamilton, Ontario, Canada, Aug. 17-18, 1981, pp. 161 - 163.
6. L. F. Fougere, "A solution to the problem of spontaneous line splitting in maximum entropy power spectrum analysis," J. Geophys. vol. 82, no. 2, pp. 1051-1054, March 1977.
7. W. Y. Chen and G. R. Stegen, "Experiments with maximum entropy power spectra of sinusoids," J. Geophys. vol. 79, pp. 3019-3022, 1974.
8. E. A. Robinson, "Multichannel Time Series Analysis with Digital Computer Programs," Holden-Day, 1967.
9. R. A. Wiggins and E. A. Robinson, "Recursive solution to the multichannel filtering problem," J. Geophys. vol. 70, pp. 1885-1891, 1965.
10. C. H. Chen and Chisung Yen, "On multichannel (multivariate) maximum entropy spectral analysis," Technical Report, SMU-EE-TR-81-2, January 23, 1981.
11. J. Makhoul, "Linear prediction: a tutorial review," Proc. IEEE, vol. 63, no. 4, pp. 561-579, 1975.
12. T. J. Ulrych and T. N. Bishop, "Maximum entropy spectral analysis and autoregressive decomposition," Rev. Geophys. Space Phys., vol. 13, no. 1, pp. 183-200, 1975.

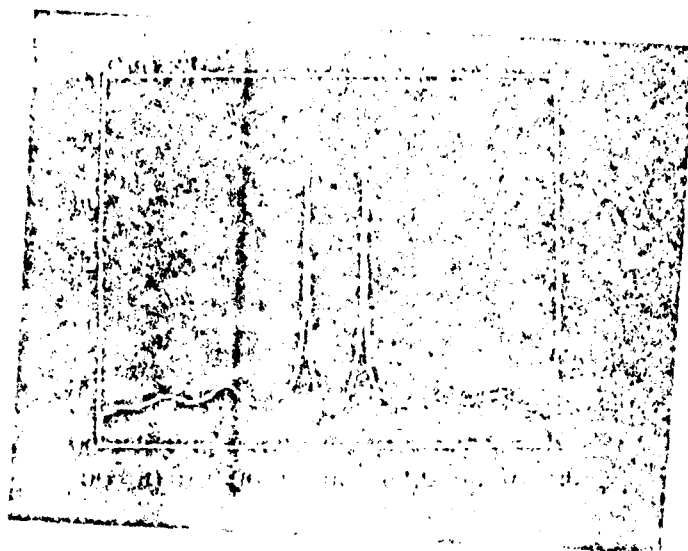


Fig. 1a 1-1 spectrum, $|S_{11}(f)|$, for real signal.

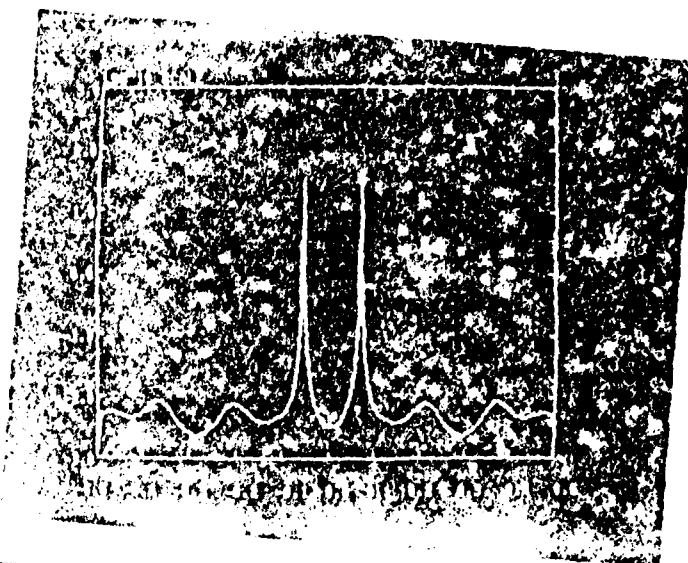


Fig. 2a 1-2 Spectrum, $|S_{12}(f)|$, for real signal.

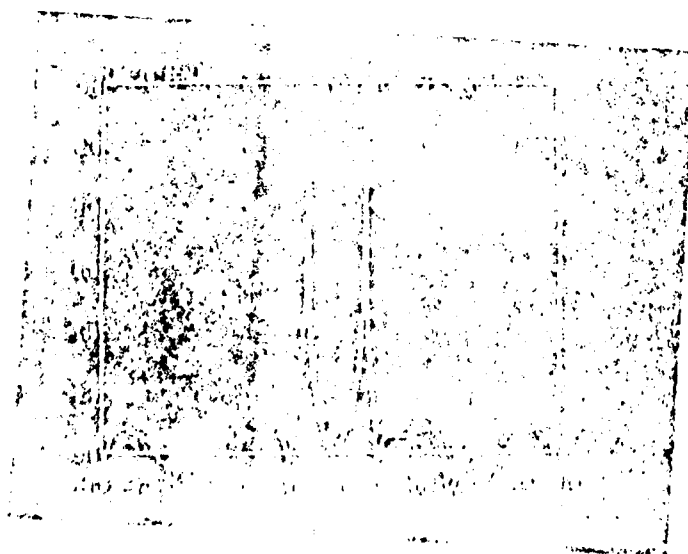


Fig. 1b Absolute value of 1-2 spectrum $|S_{12}(f)|$ for real signal.

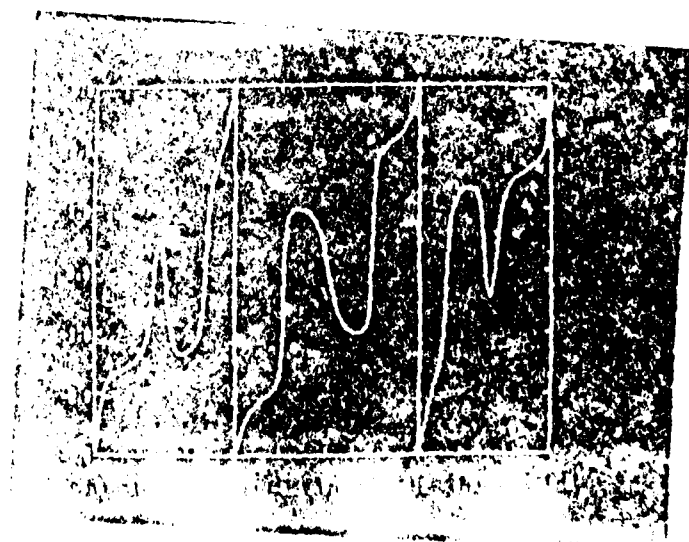


Fig. 2b Phase of 1-2 spectrum, $\arg S_{12}(f)$ for real signal.

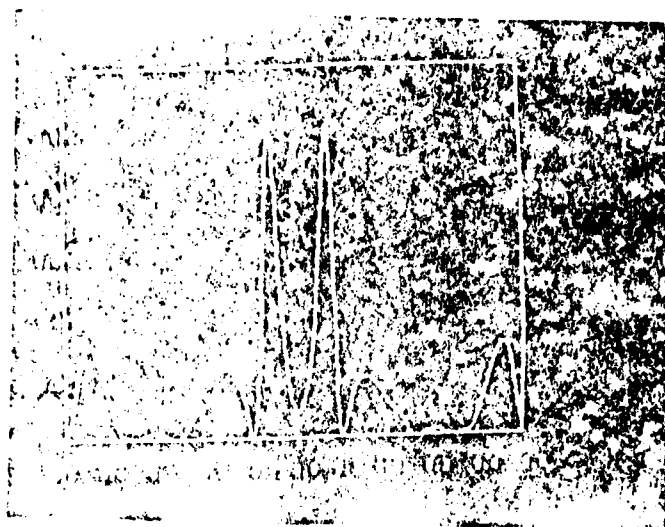


Fig. 2b 1- σ spectrum coherence squared, for real signal.

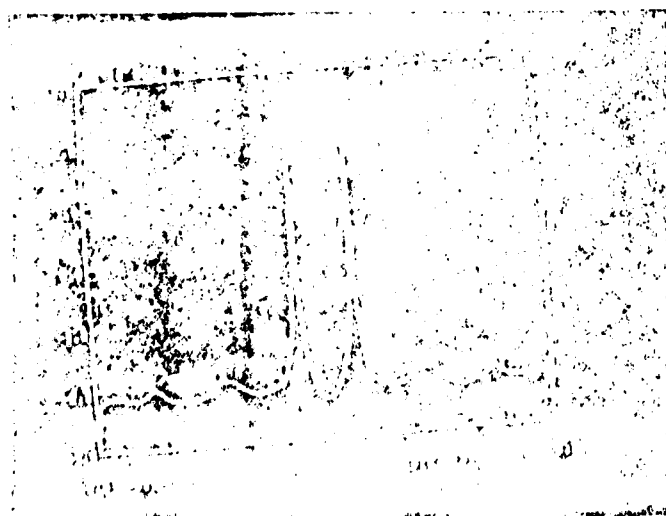


Fig. 2f Maximum eigenvalues of spectrum for real signal.

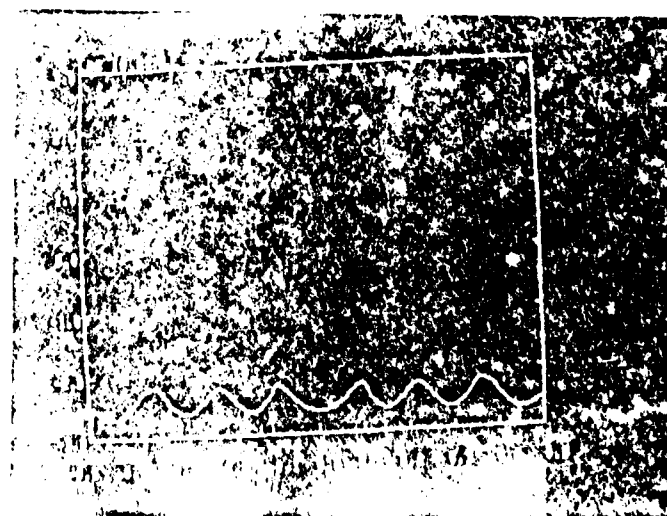


Fig. 2g Minimum eigenvalues of spectrum for real signal.

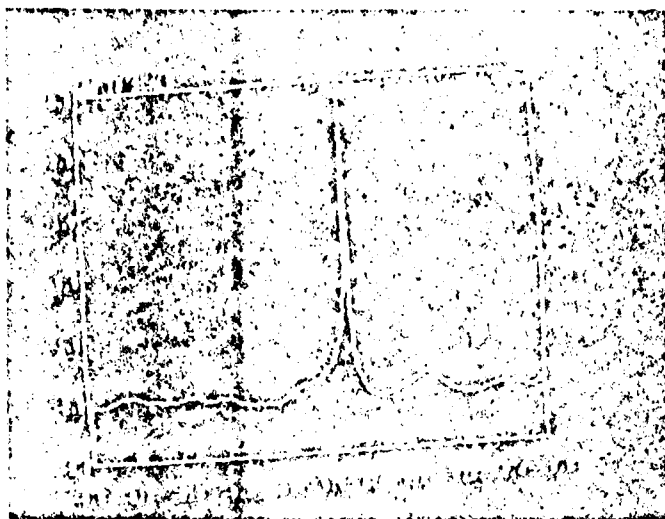


Fig. 3a 1-1 spectrum, $S_{11}(f)$ for complex signal.

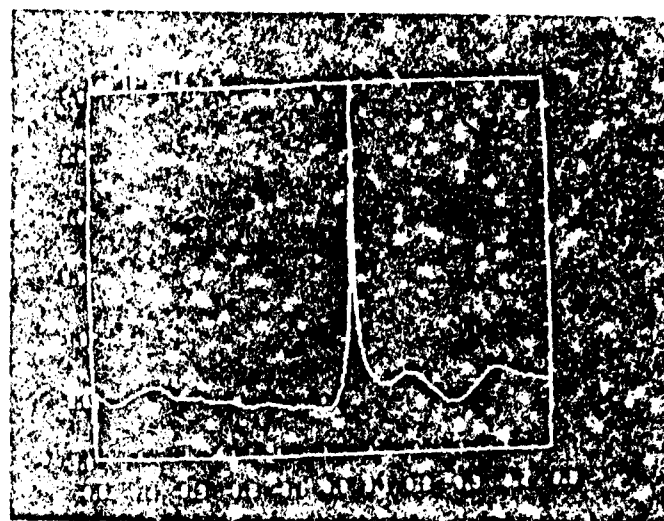


Fig. 3b 2-2 spectrum, $S_{22}(f)$ for complex signal.

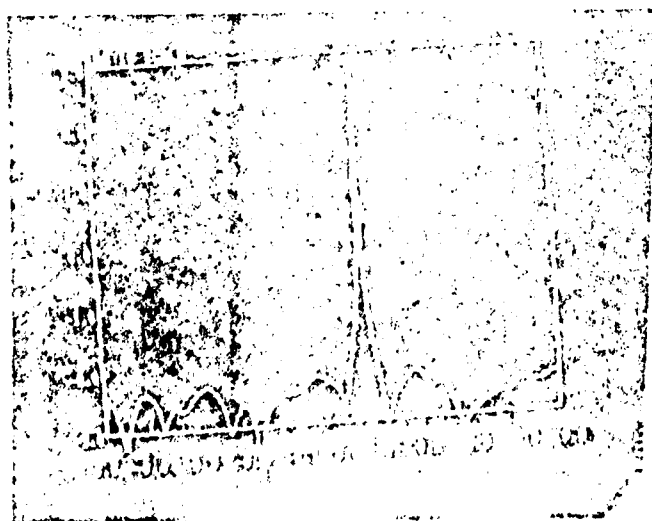


Fig. 3c Absolute value of 1-2 spectrum $|S_{12}(f)|$ for complex signal.

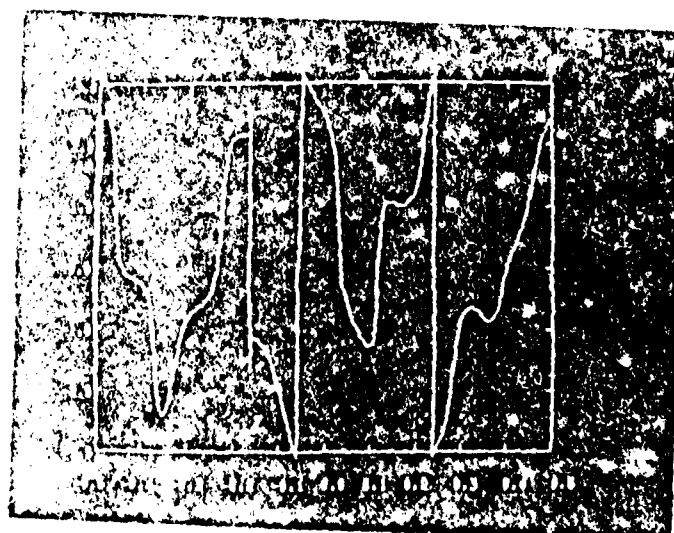


Fig. 3d Phase of 1-2 spectrum $\arg S_{12}(f)$ for complex signal.

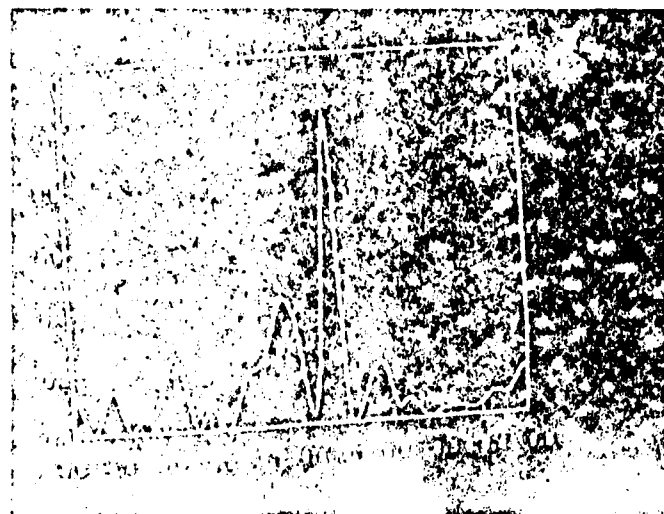


Fig. 56 1-1 spectrum coherence squared for complex signal.

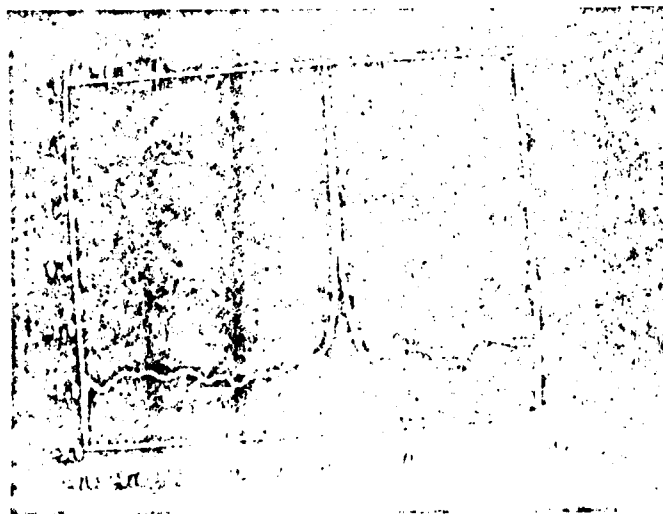


Fig. 57 Maximum eigenvalues of spectrum for complex signal.



Fig. 58 Minimum eigenvalues of spectrum for complex signal.

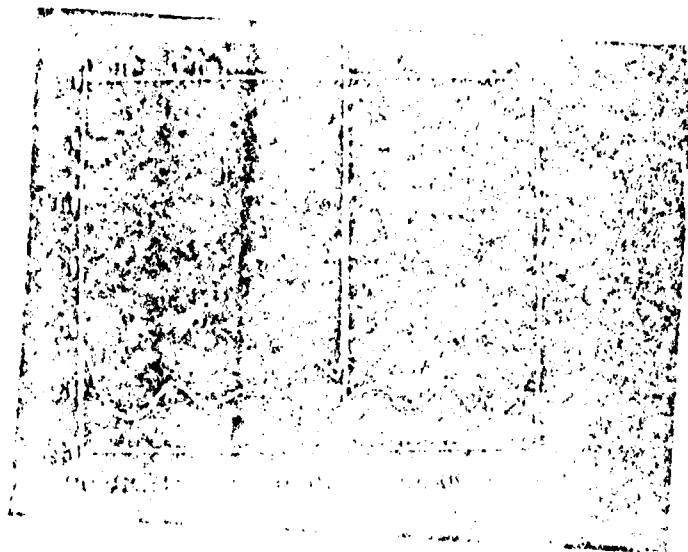


Fig. 4a 1-1 spectrum, $S_{11}(f)$ for complex signal.

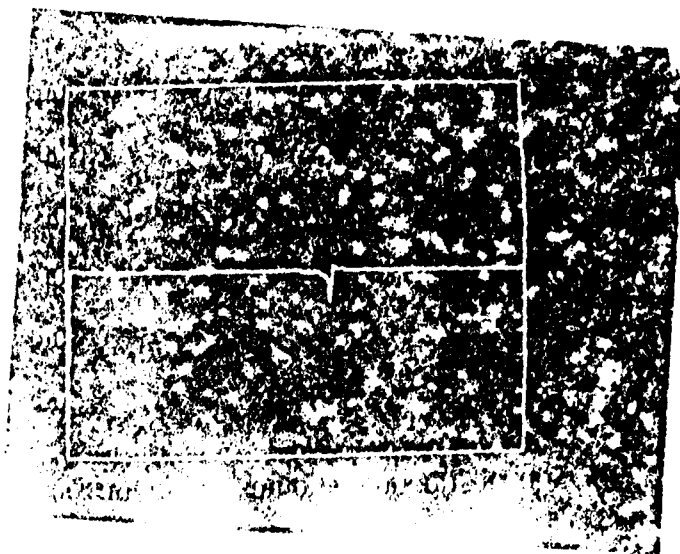


Fig. 4b phase of 1-2 spectrum, $\arg S_{12}(f)$ for complex signal. Given freq. = 0.00 Hz and phase diff. = 0.5 rad.

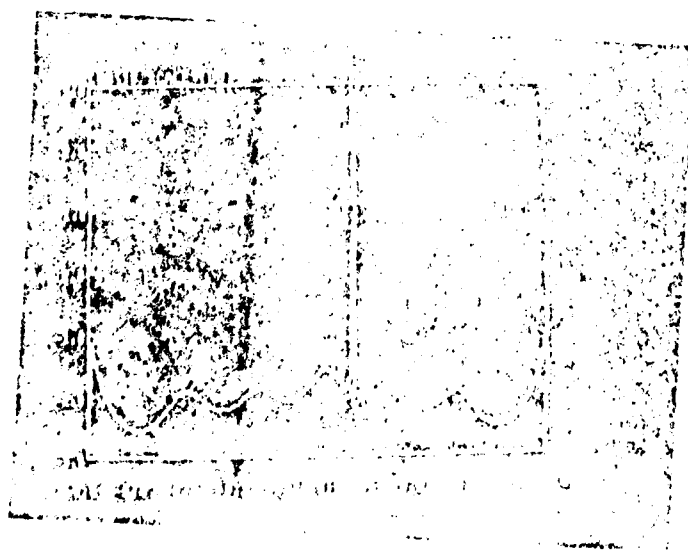


Fig. 5a 1-1 spectrum, $S_{11}(f)$ for complex signal.

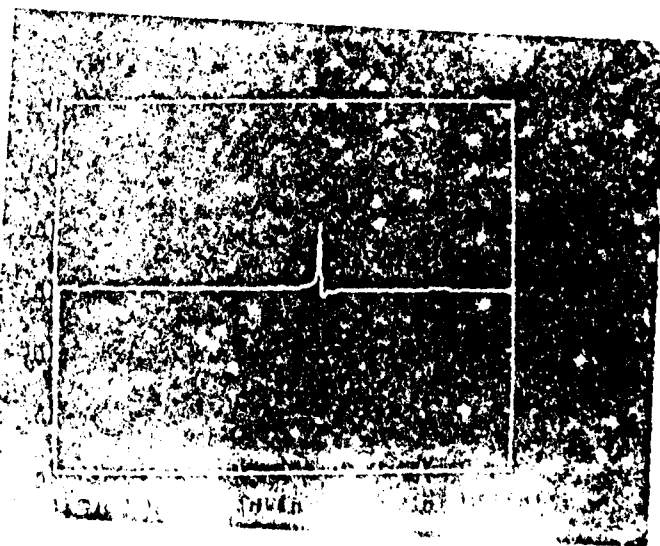


Fig. 5b phase of 1-2 spectrum, $\arg S_{12}(f)$ for complex signal. Given freq. = 0.0025 Hz and phase diff. = -1 rad.

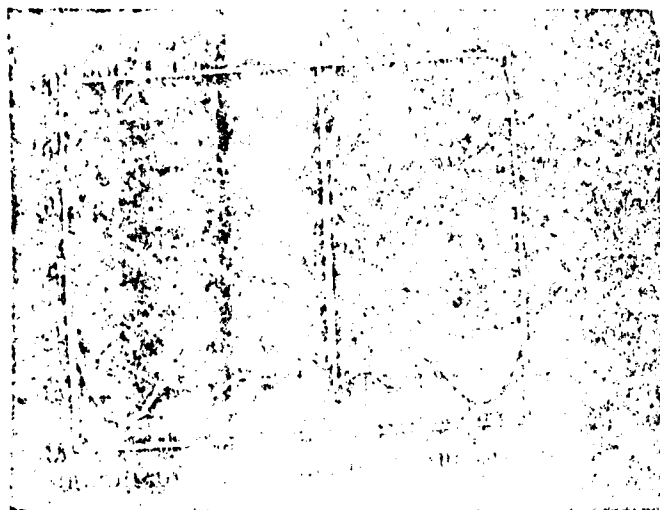


Fig. 6a 1-1 spectrum $S_{11}(f)$ for complex signal.

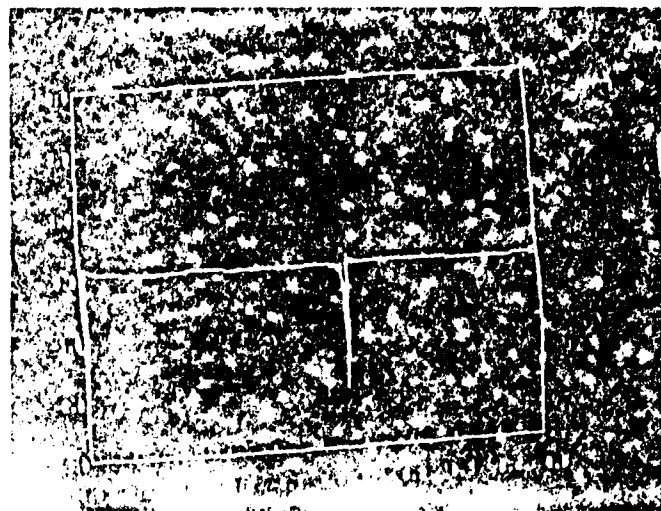


Fig. 6b phase of 1-2 spectrum, and $S_{12}(f)$ for complex signal, given freq.=0.5 Hz, and phase diff.=2 rad.

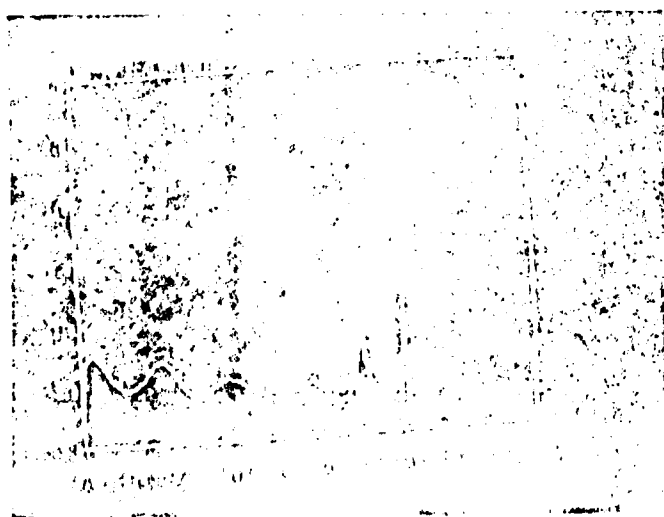


Fig. 7a 1-1 spectrum $S_{11}(f)$ for complex signal.

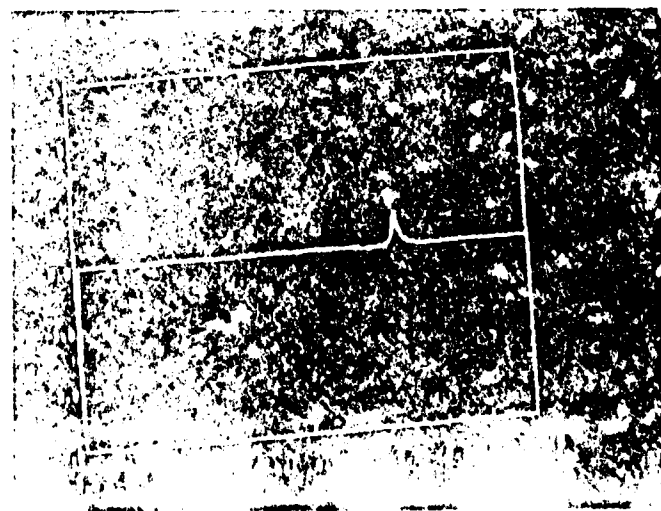


Fig. 7b phase of 1-2 spectrum, and $S_{12}(f)$ for complex signal, given freq.=0.5 Hz, and phase diff.=0.5 rad.

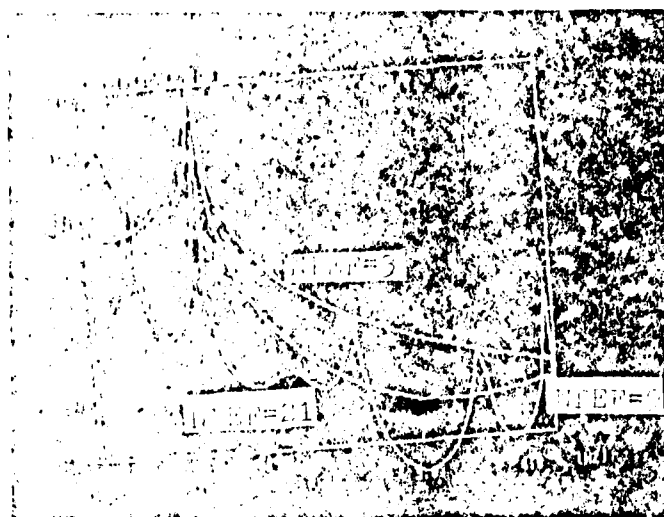


Fig. 1a Maximum energy power spectra
of 1-channel road data.
($R_1=0$, $\lambda=0.05$, $R_0=24$, $\ln P=3$,
 $\sigma, 21$).

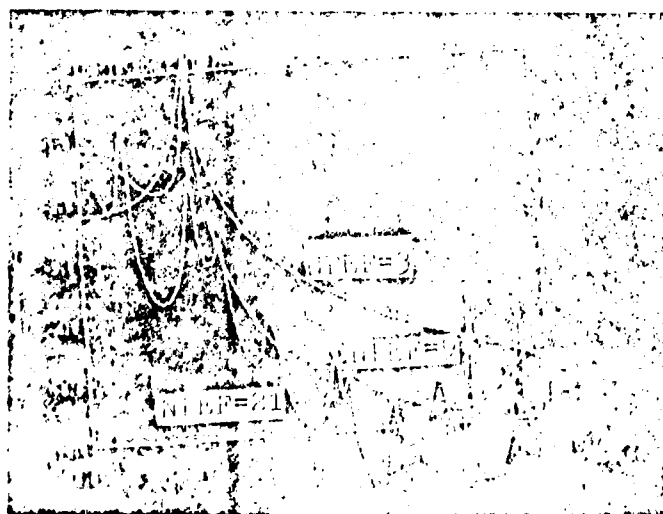


Fig. 1b Maximum energy power spectra
of 2-channel road data.
($R_1=0$, $\lambda_1=1.0$, $\lambda=0.05$,
 $R_0=24$, $\ln P=3$, $\sigma, 21$).

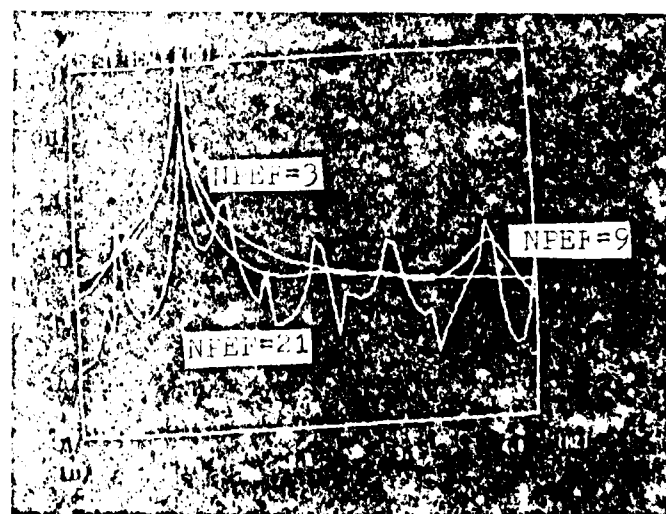


Fig. 1c Same as Fig. 1b but with
complex signals.

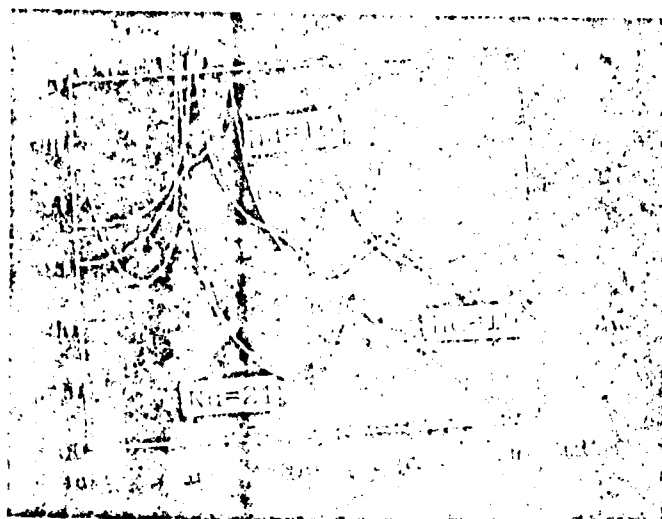


Fig. 9a Maximum entropy power spectra
for 1-channel real data.
($b_1=0$, $a_1=1.0$, $A=0.05$,
BER=9, $N_d=19, 21, 23$)

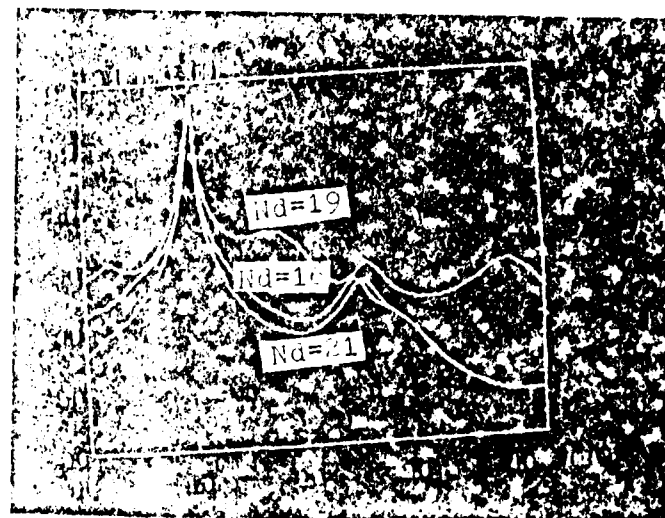


Fig. 9b Same as Fig. 9a but with
complex signals.

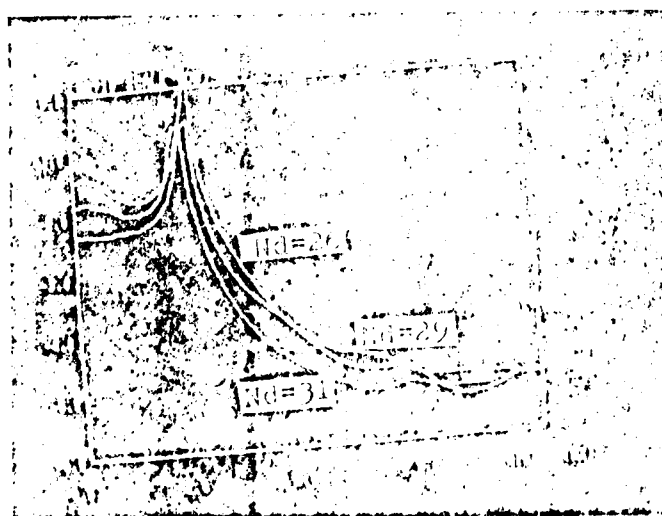


Fig. 10a Maximum entropy power spectra
for 1-channel real data.
($b_1=0$, $a_1=1.0$, $A=0.05$,
BER=9, $N_d=26, 29, 31$)

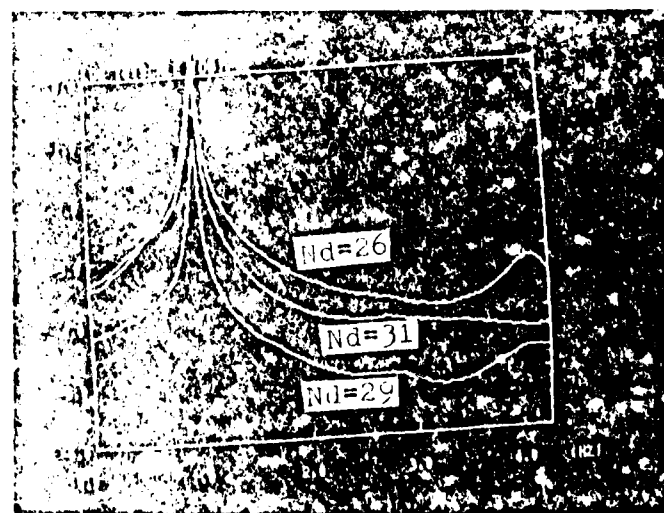


Fig. 10b Same as Fig. 10a, but with
complex signals.



Fig. 11a Maximum entropy power spectrum of 2-channel real data.
 $(\alpha_1=0, \alpha_2=1.0, A=0.05, R=2, N_d=30, 36, 41)$

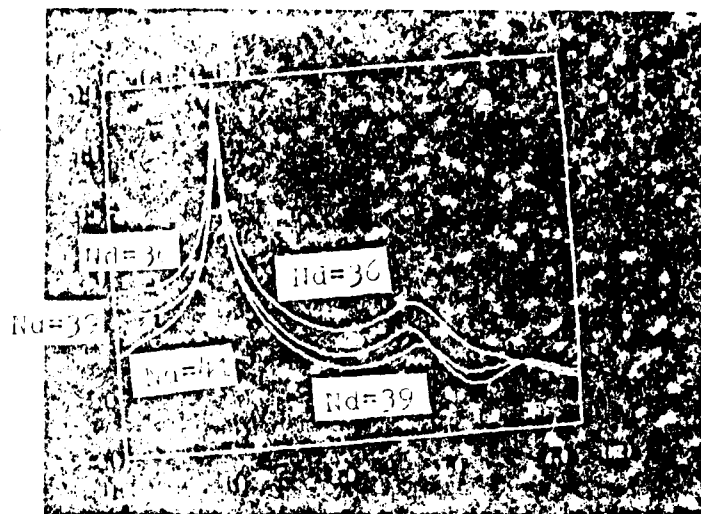


Fig. 11b Same as Fig. 11a but with complex signals.

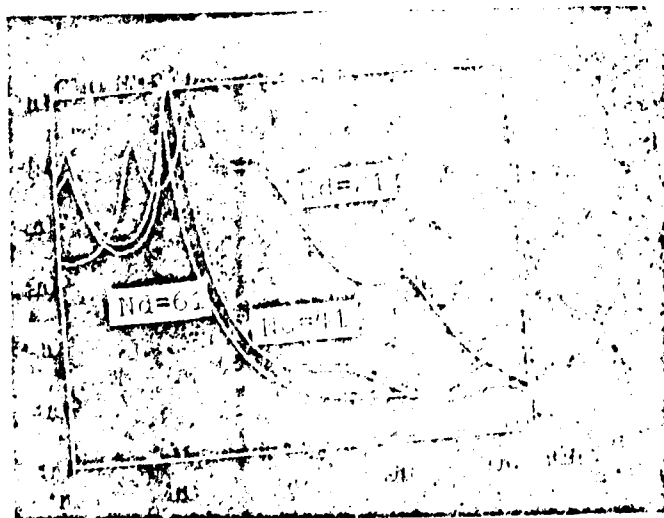


Fig. 12a Maximum entropy power spectrum of 2-channel real data.
 $(\alpha_1=48, \alpha_2=13, A=0.05, R=2, N_d=21, 41, 61)$

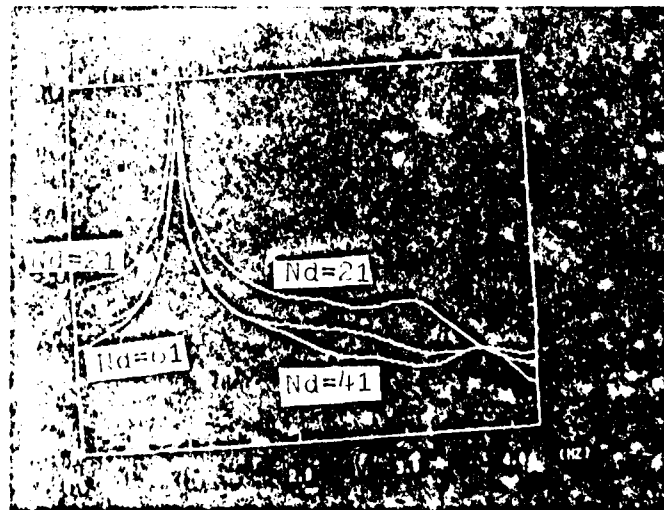


Fig. 12b Same as Fig. 12a but with complex signals.

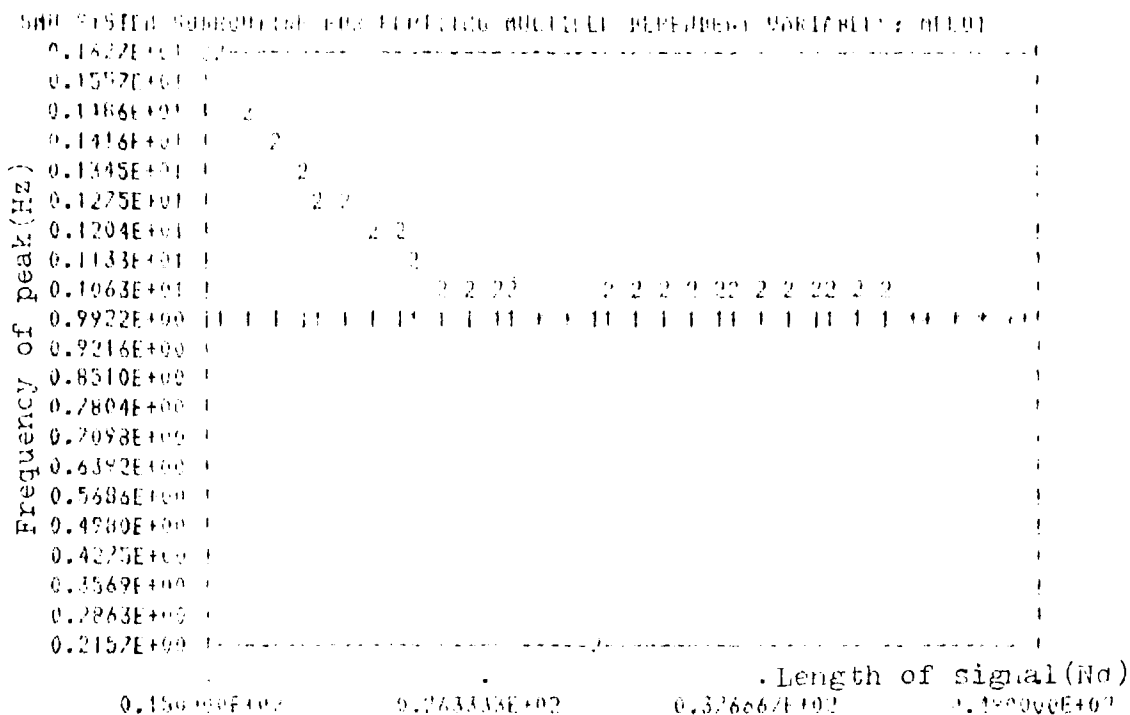


Fig. 15 The location of spectral peak for various lengths of 1Hz sinusoids. "1" denotes complex signals, "2" denotes real signals, and "*" denotes both "1" and "2" ($\phi_1=45, \phi_2=135, A=0.05, NPEF=9$)

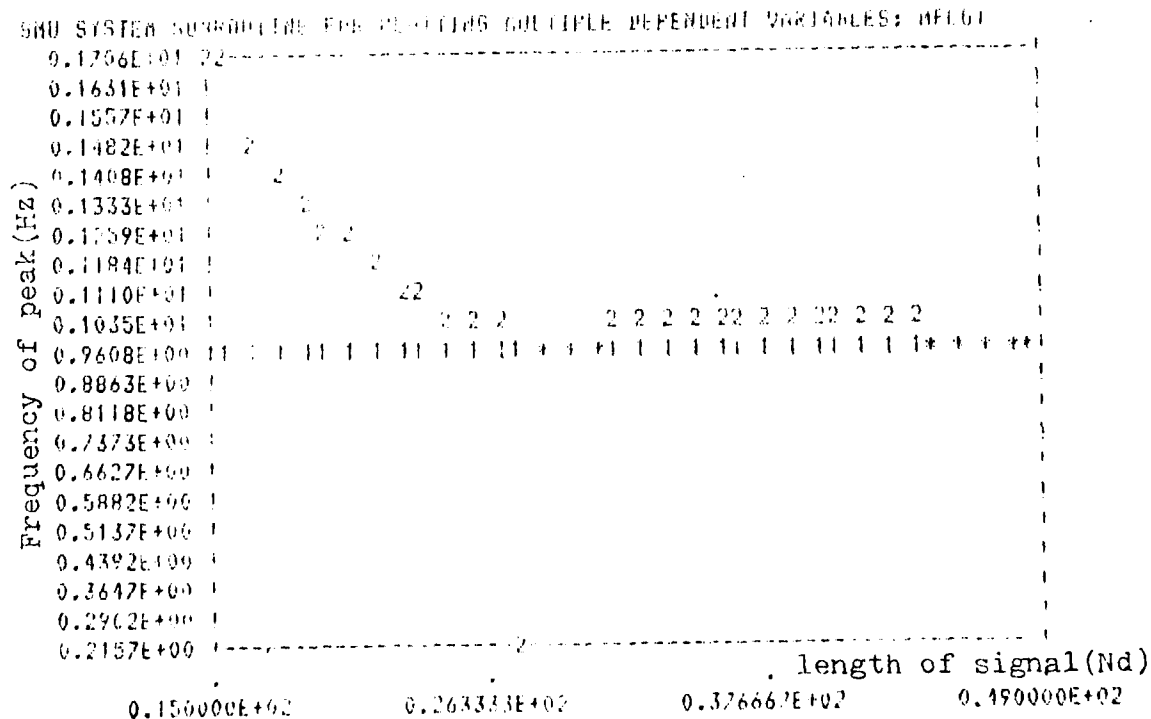


Fig. 16 Same as Fig. 14 but with $\phi_1=-45, \phi_2=-135, A=0.05, NPEF=9$.

Appendix Computer Program for the Multichannel Channel Maximum Entropy Spectral Analysis

```

C THE FILE: CHAN.FOR
C*****
C
C      PROGRAM MAXIMUM ENTROPY ROUTINE
C      FOR (GENERAL) P-CHANNEL, COMPLEX.
C
C      ARGUMENTS:
C
C      NC = MAX. FILTER LENGTH.
C      NP = # OF CHANNELS.
C      NSPE = MIN. FILTER LENGTH (DESIRED SPECTRUM).
C      NDAT = # OF DATA POINTS.
C      NPRS = MIN. FILTER LENGTH (DESIRED PRINTOUT).
C
C      INPUT DATA IS STORED IN FILE 'SIN.DAT'.
C
C      THIS PROGRAM MUST LINK WITH THE FOLLOWING SUBROUTINES:
C      DRAW      PROGRAM TO DISPLAY THE DESIRED DATA
C               ON THE TERMINAL.
C      PLOTCH
C      EIGEN      SUBROUTINES OF THIS SOFTWARE PACKAGE.
C
C*****
C      COMMON /P/PI,DI,NDAT,NP
C      COMMON /M/NO
C      COMMON /S/EL,TS,S
C      COMMON /K/IN,NPRS
C      DIMENSION YI(1,300)
C      DIMENSION UU(4),VV(4)
C      COMPLEX YI
C      TYPE 1110
1110   FORMAT(2X,1/P,NC,NP,NSPE,NDAT,NPRS,DI)
C      ACCEPT 1,NC,NP,NSPE,NDAT,NPRS,DI
C      TYPE 4
4   FORMAT(//)
C      TYPE 11,NC,NP
11  FORMAT(1X,27HMAX. NO. OF FILTER COEFF. =,115.2X,41HNO. OF COMPONE
      THIS IS VECTOR TIME SERIES =,115.//)
C      TYPE 2,NDAT,DI
2   FORMAT(1X,24HORIGINAL TIME SERIES HAS,117.2X,28HDATA POINTS AT TI
      ME INTERVAL,1F10.5,/)
C      OPEN(UNIT=50,FILE='SIN.DAT')
C      DO 2 K=1,NDAT
C      READ (30.20)(UU(I),VV(I),I=1,NP)
20  FORMAT(4F10.3)
C      DO 3 I=1,NP
3   YI(I,K)=CMPLX(UU(I),VV(I))
2   CONTINUE
C      CALL DEIGEN
C      CALL CALFIL
C      CALL EXIT
C      END

```

[illegible]


```

      SUBROUTINE CUBIC
      COMMON /CUBIC/ A(10), B(10), C(10), D(10), E(10), F(10), G(10), H(10), I(10), J(10)
      COMMON /CUBIC/ K(10), L(10), M(10), N(10), O(10), P(10), Q(10), R(10), S(10), T(10)
      COMMON /CUBIC/ U(10), V(10), W(10), X(10), Y(10), Z(10), AA(10), AB(10), AC(10), AD(10)
      COMMON /CUBIC/ AE(10), AF(10), AG(10), AH(10), AI(10), AJ(10), AK(10), AL(10), AM(10), AN(10)
      COMMON /CUBIC/ AO(10), AP(10), AQ(10), AR(10), AS(10), AT(10), AU(10), AV(10), AW(10), AX(10)
      COMMON /CUBIC/ AY(10), AZ(10), BA(10), BB(10), BC(10), BD(10), BE(10), BF(10), BG(10), BH(10)
      COMMON /CUBIC/ BI(10), BJ(10), BK(10), BL(10), BM(10), BN(10), BO(10), BP(10), BQ(10), BR(10)
      COMMON /CUBIC/ BS(10), BT(10), BU(10), BV(10), BW(10), BX(10), BY(10), BZ(10), CA(10), CB(10)
      COMMON /CUBIC/ CC(10), CD(10), CE(10), CF(10), CG(10), CH(10), CI(10), CJ(10), CK(10), CL(10)
      COMMON /CUBIC/ CM(10), CN(10), CO(10), CP(10), CQ(10), CR(10), CS(10), CT(10), CU(10), CV(10)
      COMMON /CUBIC/ CW(10), CX(10), CY(10), CZ(10), DA(10), DB(10), DC(10), DD(10), DE(10), DF(10)
      COMMON /CUBIC/ DG(10), DH(10), DI(10), DJ(10), DK(10), DL(10), DM(10), DN(10), DO(10), DP(10)
      COMMON /CUBIC/ EQ(10), ER(10), ES(10), ET(10), EU(10), EV(10), EW(10), EX(10), EY(10), EZ(10)
      COMMON /CUBIC/ FA(10), FB(10), FC(10), FD(10), FE(10), FF(10), FG(10), FH(10), FI(10), FJ(10)
      COMMON /CUBIC/ FK(10), FL(10), FM(10), FN(10), FO(10), FP(10), FQ(10), FR(10), FS(10), FT(10)
      COMMON /CUBIC/ FU(10), FV(10), FW(10), FX(10), FY(10), FZ(10), GA(10), GB(10), GC(10), GD(10)
      COMMON /CUBIC/ GE(10), GF(10), GH(10), GI(10), GJ(10), GK(10), GL(10), GM(10), GN(10), GO(10)
      COMMON /CUBIC/ GP(10), GQ(10), GR(10), GS(10), GT(10), GU(10), GV(10), GW(10), GX(10), GY(10)
      COMMON /CUBIC/ GZ(10), HA(10), HB(10), HC(10), HD(10), HE(10), HF(10), HG(10), HH(10), HI(10)
      COMMON /CUBIC/ HJ(10), HK(10), HL(10), HM(10), HN(10), HO(10), HP(10), HQ(10), HR(10), HS(10)
      COMMON /CUBIC/ HT(10), HU(10), HV(10), HW(10), HX(10), HY(10), HZ(10), IA(10), IB(10), IC(10), ID(10)
      COMMON /CUBIC/ IE(10), IF(10), IG(10), IH(10), II(10), IJ(10), IK(10), IL(10), IM(10), IN(10)
      COMMON /CUBIC/ IO(10), IP(10), IQ(10), IR(10), IS(10), IT(10), IU(10), IV(10), IW(10), IX(10)
      COMMON /CUBIC/ IY(10), IZ(10), JA(10), JB(10), JC(10), JD(10), JE(10), JF(10), JG(10), JH(10)
      COMMON /CUBIC/ JJ(10), JK(10), JL(10), JM(10), JN(10), JO(10), JP(10), JQ(10), JR(10), JS(10)
      COMMON /CUBIC/ JT(10), JU(10), JV(10), JW(10), JX(10), JY(10), JZ(10), KA(10), KB(10), KC(10), KD(10)
      COMMON /CUBIC/ KE(10), KF(10), KG(10), KH(10), KI(10), KJ(10), KK(10), KL(10), KM(10), KN(10)
      COMMON /CUBIC/ KO(10), KP(10), KQ(10), KR(10), KS(10), KT(10), KU(10), KV(10), KW(10), KX(10)
      COMMON /CUBIC/ KY(10), KZ(10), LA(10), LB(10), LC(10), LD(10), LE(10), LF(10), LG(10), LH(10)
      COMMON /CUBIC/ LI(10), LJ(10), LK(10), LL(10), LM(10), LN(10), LO(10), LP(10), LQ(10), LR(10)
      COMMON /CUBIC/ LS(10), LT(10), LU(10), LV(10), LW(10), LX(10), LY(10), LZ(10), MA(10), MB(10)
      COMMON /CUBIC/ MC(10), MD(10), ME(10), MF(10), MG(10), MH(10), MI(10), MJ(10), MK(10), ML(10)
      COMMON /CUBIC/ MM(10), MN(10), MO(10), MP(10), MQ(10), MR(10), MS(10), MT(10), MU(10), MV(10)
      COMMON /CUBIC/ MW(10), MX(10), MY(10), MZ(10), NA(10), NB(10), NC(10), ND(10), NE(10), NF(10)
      COMMON /CUBIC/ NG(10), NH(10), NI(10), NJ(10), NK(10), NL(10), NM(10), NN(10), NO(10), NP(10)
      COMMON /CUBIC/ OQ(10), OR(10), OS(10), OT(10), OU(10), OV(10), OW(10), OX(10), OY(10), OZ(10)
      COMMON /CUBIC/ PA(10), PB(10), PC(10), PD(10), PE(10), PF(10), PG(10), PH(10), PI(10), PJ(10)
      COMMON /CUBIC/ PK(10), PL(10), PM(10), PN(10), PO(10), PP(10), PQ(10), PR(10), PS(10), PT(10)
      COMMON /CUBIC/ PU(10), PV(10), PW(10), PX(10), PY(10), PZ(10), QA(10), QB(10), QC(10), QD(10)
      COMMON /CUBIC/ QE(10), QF(10), QG(10), QH(10), QI(10), QJ(10), QK(10), QL(10), QM(10), QN(10)
      COMMON /CUBIC/ QO(10),QP(10), QQ(10), QR(10), QS(10), QT(10), QU(10), QV(10), QW(10), QX(10)
      COMMON /CUBIC/ QY(10), QZ(10), RA(10), RB(10), RC(10), RD(10), RE(10), RF(10), RG(10), RH(10)
      COMMON /CUBIC/ RI(10), RJ(10), RK(10), RL(10), RM(10), RN(10), RO(10), RP(10), RQ(10), RR(10)
      COMMON /CUBIC/ RS(10), RT(10), RU(10), RV(10), RW(10), RX(10), RY(10), RZ(10), SA(10), SB(10)
      COMMON /CUBIC/ SC(10), SD(10), SE(10), SF(10), SG(10), SH(10), SI(10), SJ(10), SK(10), SL(10)
      COMMON /CUBIC/ SM(10), SN(10), SO(10), SP(10), SQ(10), SR(10), SS(10), ST(10), SU(10), SV(10)
      COMMON /CUBIC/ SW(10), SX(10), SY(10), SZ(10), TA(10), TB(10), TC(10), TD(10), TE(10), TF(10)
      COMMON /CUBIC/ TG(10), TH(10), TI(10), TJ(10), TK(10), TL(10), TM(10), TN(10), TO(10), TP(10)
      COMMON /CUBIC/ TQ(10), TR(10), TS(10), TT(10), TU(10), TV(10), TW(10), TX(10), TY(10), TZ(10)
      COMMON /CUBIC/ UA(10), UB(10), UC(10), UD(10), UE(10), UF(10), UG(10), UH(10), UI(10), UJ(10)
      COMMON /CUBIC/ UK(10), UL(10), UM(10), UN(10), UO(10), UP(10), UQ(10), UR(10), US(10), UT(10)
      COMMON /CUBIC/ UU(10), UV(10), UW(10), UX(10), UY(10), UZ(10), VA(10), VB(10), VC(10), VD(10)
      COMMON /CUBIC/ VE(10), VF(10), VG(10), VH(10), VI(10), VJ(10), VK(10), VL(10), VM(10), VN(10)
      COMMON /CUBIC/ VO(10), VP(10), VQ(10), VR(10), VS(10), VT(10), VU(10), VV(10), VW(10), VX(10)
      COMMON /CUBIC/ VY(10), VZ(10), WA(10), WB(10), WC(10), WD(10), WE(10), WF(10), WG(10), WH(10)
      COMMON /CUBIC/ WI(10), WJ(10), WK(10), WL(10), WM(10), WN(10), WO(10), WP(10), WQ(10), WR(10)
      COMMON /CUBIC/ WS(10), WT(10), WU(10), WV(10), WW(10), WX(10), WY(10), WZ(10), XA(10), XB(10)
      COMMON /CUBIC/ XC(10), XD(10), XE(10), XF(10), XG(10), XH(10), XI(10), XJ(10), XK(10), XL(10)
      COMMON /CUBIC/ XM(10), XN(10), XO(10), XP(10), XQ(10), XR(10), XS(10), XT(10), XU(10), XV(10)
      COMMON /CUBIC/ XW(10), XX(10), XY(10), XZ(10), YA(10), YB(10), YC(10), YD(10), YE(10), YF(10)
      COMMON /CUBIC/ YG(10), YH(10), YI(10), YJ(10), YK(10), YL(10), YM(10), YN(10), YO(10), YP(10)
      COMMON /CUBIC/ YQ(10), YR(10), YS(10), YT(10), YU(10), YV(10), YW(10), YX(10), YY(10), YZ(10)
      COMMON /CUBIC/ ZA(10), ZB(10), ZC(10), ZD(10), ZE(10), ZF(10), ZG(10), ZH(10), ZI(10), ZJ(10)
      COMMON /CUBIC/ ZK(10), ZL(10), ZM(10), ZN(10), ZO(10), ZP(10), ZQ(10), ZR(10), ZS(10), ZT(10)
      COMMON /CUBIC/ ZU(10), ZV(10), ZW(10), ZX(10), ZY(10), ZZ(10)
      COMMON /CUBIC/ AAA(10), AAB(10), AAC(10), AAD(10), AAU(10), AAV(10), AAW(10), AAX(10), AAY(10), AAZ(10)
      COMMON /CUBIC/ ABA(10), ABB(10), ABC(10), ABD(10), ABU(10), ABV(10), ABW(10), ABX(10), ABY(10), ABZ(10)
      COMMON /CUBIC/ ACA(10), ACB(10), ACC(10), ACD(10), ACU(10), ACV(10), ACW(10), ACX(10), ACY(10), ACZ(10)
      COMMON
```



```

      DO 10 J=1,NP
20  FFS(1,J)=0.0
      DO 10 I=1,NP
      DO 10 J=1,NP
      DO 10 K=1,NP
28  F1=0.0,J)=FFS(1,J,K)
      CALL COMBINE10V,NP,BFB)
      DO 10 I=1,NP
      DO 10 J=1,NP
      V33(1,J)=COMPLX(0.,0.)
      DO 10 KK=1,NP
29  V33(1,J)=V33(1,J)+E10V(1,KK)*F(KK,J)
      DO 10 I=1,NP
      DO 10 J=1,NP
      V44(1,J)=COMPLX(0.,0.)
      DO 10 KK=1,NP
31  V11(1,J)=V44(1,J)+V33(1,KK)+CONJG(E10V(1,KK))
30  FFS(1,J)=V44(1,J)*D1
27  CONTINUE
      DO 30 K=1,NBP1
      GRN1=FLGRN(K-1)
36  FREGR(K)=RTT*GRN1
      DO 30 I=1,N3
      LGR=FLGRN(K-1-N3)
      D1PR=H34K
32  E1=0.0,GRN1)=0.0,FREGR)
      DO 30 M=1,N5
      D1PR=D1PR*E1
      X1=0.0,FREGR)
      X1=0.0,FREGR)
      DO 30 I=1,NP
      DO 30 J=1,NP
      V52(1,J)=FFS(1,I,K)
      V53(1,J)=FFS(1,I,NBP6)
      V54(1,J,K)=V55(1,J)
34  FFS(1,J)=V53(1,J)+V54(1,J)
      CALL COMBINE10V,NP1
38  FFS(1,J)=XK2
      TYPE 35
33  FGRN(1,J)
      DO 30 K=1,N2
      DO 30 I=1,NP
39  GRN(1)=SCAL(FFS(1,I,K))
      DO 30 I=1,NP
      TYPE 39,1,1
37  FOURGR(1,1,10.,11.,11.,11)=POWER SPECTRUM BELOW,2)
      TYPE 41
      CALL DRGR(5,11,1)
      TYPE 41,GRN(1,K=1,42)
41  FOURGR(1,10E15,5)
      TYPE 42
30  CONTINUE
      TYPE 42
42  FOURGR(1,2)
      IF(GR(50,1169) .GT. 5)
      NPA1=NP-1
      DO 82 I=1,NPB1)
      IF1=1+1

```



```

      DO 43 I=1,NP
      DO 44 J=1,NM1
      V4R(1,J)=REAL(B1(1,J))
43  V4I(1,J)=AIMAG(B1(1,J))
      DO 45 I=1,NP
      TYPE 11
      TYPE 8
      TYPE 8,(V4R(1,J),J=1,NM1)
      TYPE 9
      TYPE 10
      TYPE 8,(V4I(1,J),J=1,NM1)
      TYPE 1
44  CONTINUE
      TYPE 11
11  FORMAT(10X,14HE-MATRIX BELOW,/)
      DO 12 I=1,NP
      DO 12 J=1,NP
      V4R(1,J)=REAL(C(1,J))
12  V4I(1,J)=AIMAG(C(1,J))
      TYPE 1
      TYPE 13,((V4R(1,J),J=1,NP),I=1,NP)
13  FORMAT(12Z0.10)
      TYPE 10
      TYPE 13,((V4I(1,J),J=1,NP),I=1,NP)
      TYPE 9
      IR=0.
      DO 15 I=1,NP
45  IR=IR+V4R(1,I)
      TYPE 17,IR
47  FORMAT(10X,7HTRACE =,1E20.10,/)
      TYPE 14
14  FORMAT(10X,14HE-MATRIX BELOW,/)
      DO 15 I=1,NP
      DO 15 J=1,NP
      V4R(1,J)=REAL(G(1,J))
15  V4I(1,J)=AIMAG(G(1,J))
      TYPE 8
      TYPE 13,((V4R(1,J),J=1,NP),I=1,NP)
      TYPE 10
      TYPE 13,((V4I(1,J),J=1,NP),I=1,NP)
      TYPE 2
      TYPE 16
16  FORMAT(10X,14HE-MATRIX BELOW,/)
      DO 17 I=1,NP
      DO 17 J=1,NP
      V4R(1,J)=REAL(A(1,J))
17  V4I(1,J)=AIMAG(A(1,J))
      TYPE 6
      TYPE 13,((V4R(1,J),J=1,NP),I=1,NP)
      TYPE 10
      TYPE 13,((V4I(1,J),J=1,NP),I=1,NP)
      TYPE 7
      IR=0.
      DO 46 I=1,NP
46  IR=IR+V4R(1,I)
      TYPE 17,IR
      TYPE 18
18  FORMAT(1X,26HFORWARD POWER MATRIX BELOW,/)

```



```

CALL F16CHGE16,HP,4,AE16)
CALL F16CHGE16,HP,0,EL,VI,4,WK,IER)
STOP
GO TO 11,91
51 TYPE 30,EL(1)
TYPE 30
30 FORMAT(1X,2HEIGENVALUES OF P BELOW,/)
TYPE 13,EL(1),I=1,HP)
TYPE 30
TYPE 30,30X
80 CONTINUE
GO 92 I=1,HP
GO 92 J=1,HP
92 AE16(1,1)=P(1,1)
CALL DGVCHGE16,HP,1,AE16)
CALL F16CHGE16,HP,0,EL,VI,4,WK,IER)
IF(EL(1).LT.0.760) GO 94
GO TO 95
94 TYPE 30
96 FORMAT(1X,40MATRIX NOT POSITIVE DEFINITE--PROGRAM TERMINATED,/)
TYPE 30,EL(1)
97 FORMAT(1X,2HEIGENVALUE -, (E10.10)
STOP
98 CONTINUE
STOP
      DETP(IEP)=1.
      ELP(IEP,1)=EL(HP)
      ELP(IEP,2)=EL(1)
GO 62 I=1,HP
DETP(IEP)=DETP(IEP)*EL(1)
62 SUB=SUB+EL(1)
FACT=(ALPHA+EL(HP))/((FACT)-1.)*EOLD)
DEP(IEP)=DETP(IEP)*(FACT*HP)
IF(19.11.DPRS)GO TO 81
TYPE 33
33 FORMAT(1X,2HEIGENVALUES OF P BELOW,/)
TYPE 13,EL(1),I=1,HP)
TYPE 30,30X
TYPE 30
81 CONTINUE
GO 93 I=1,HP
GO 93 J=1,HP
93 AE16(1,1)=P(1,1)
CALL DGVCHGE16,HP,4,AE16)
CALL F16CHGE16,HP,0,EL,VI,4,WK,IER)
IF(EL(1).LT.0.060) GO 104
GO TO 105
104 TYPE 30
TYPE 27,EL(1)
STOP
105 CONTINUE
STOP
      DETP(IEP)=1.
      ELPP(IEP,1)=EL(HP)
      ELPP(IEP,2)=EL(1)
GO 83 I=1,HP
DETP(IEP)=DETP(IEP)*EL(1)
83 SUB=SUB+EL(1)
IF(19.11.DPRS)GO TO 82
TYPE 33
33 FORMAT(1X,2HEIGENVALUES OF P PRIME BELOW,/)

```



```

    DO 12 J=1,JP
12  U1(I,J)=U1(I,J)+V1(I,K)*FF(I,J)
    DO 38 I=1,IP
    DO 39 J=1,JP
38  U10(I,J)=U1(I,J)
    CALL CHGPR(I0,IP,JP,IP2)
    DO 12 I=1,IP
    DO 39 J=1,JP
39  V1(I,J)=U10(I,J)
    DO 13 I=1,IP
    DO 13 J=1,JP
    U2(I,J)=CHPLX(0.,0.)
    V3(I,J)=CHPLX(0.,0.)
    DO 13 K=1,RP
    U2(I,J)=U2(I,J)+U1(I,K)*E(K,J)
13  U3(I,J)=U2(I,J)+U1(I,K)*U1(K,J)
    DO 14 I=1,IP
    DO 14 J=1,JP
    U(I,J)=CHPLX(0.,0.)
    V5(I,J)=CHPLX(0.,0.)
    DO 14 K=1,RP
    U(I,J)=U(I,J)+U2(I,K)*U1(K,J)
14  U5(I,J)=U5(I,J)+U(I,K)+U3(K,J)
    DO 15 I=1,IP
    DO 15 J=1,JP
    AA(I,J)=CHPLX(0.,0.)
    GG(I,J)=CHPLX(0.,0.)
    UU(I,J)=CHPLX(0.,0.)
    DO 15 I=1,JP
    AA(I,J)=AA(I,J)+U(I,I)*E(I,J)
    GG(I,J)=GG(I,J)+U(I,K)*U1(K,J)
15  U(I,J)=U(I,J)+U(I,I)*G(K,J)+U1(I,K)*U5(K,J)
    CALL G5ICH(66,88,CC,RP,CR)
    DO 25 I=1,RP
    DO 25 J=1,JP
    V1(I,J)=CHPLX(0.,0.)
    DO 25 K=1,RP
25  U1(I,J)=U1(I,J)+CORJ6(CN(K,1))*FF(I,J)
    DO 26 I=1,JP
    DO 26 J=1,JP
    U0(I,J)=CHPLX(0.,0.)
    DO 26 K=1,RP
26  U0(I,J)=U0(I,J)+U1(I,K)+V1(K,J)
    DO 27 I=1,RP
    DO 27 J=1,JP
    DO 27 K=1,IP2
    U(I,J,K)=U(I,J,K)
27  U5(I,J,K)=U(I,J,K)
    DO 3 K=1,IP2
    DO 3 I=1,JP
    DO 3 J=1,JP
    DO 3 KK=1,KP
    U(I,J,K)=U(I,J,K)+U5(I,KK,IP2KK)*CN(KK,J)
4  U(I,J,K)=U(I,J,K)+U5(I,KK,IP2KK)*CN(KK,J)
    DO 5 K=1,RP1
    DO 5 I=1,JP
    U3(I,I)=U1(I,K)
9  U3(I,2)=U1(I,K)

```

```

      DO 3 J=1,NP
      DO 4 K=1,NP
      C(1,1)=C(1,1)+CONJG(CNPK(K,1))*V(KE,1)
      5 C(1,1)=1.0+CONJG(CNPK(K,1))*V(CK,1)
      DO 6 J=1,NP
      DO 6 K=1,NP
      Q(1,J)=CMPLX(0.,0.)
      92(1,J)=CMPLX(0.,0.)
      DO 8 J=1,NP
      Q(1,J)=Q(1,J)+P(1,K)*C(K,J)
      6 Q(1,J)=Q(1,J)+P(1,K)*C(K,J)
      DO 1 J=1,NP
      DO 2 J=1,NP
      DO 2 K=1,NP
      I(1,J)=P(1,J)+CONJG(CNPK(K,1))*Q(1,J)
      7 I(1,J)=P(1,J)+CONJG(CNPK(K,1))*Q(1,J)
      RETURN
      END

```

C-----
 SUBROUTINE GETCHS(P,C,N,CH)
 DIMENSION A(4,4),B(4,4),C(1,4),CH(4,1),PC(15),AB(16,16)
 COMPLEX A,B,C,PC,CH,AB
 C THIS SUBROUTINE SOLVES THE MATRIX EQUATION $A(X) \cdot (C(X)) \cdot B = C$ FOR THE
 C VECTOR OF COEFFICIENTS, CH. THE METHOD IS THAT OF PELLER, MATRIX
 C ANALYSIS, OLD EDITION, PAGE 231.

```

      N=15
      DO 1 I=1,N
      DO 1 J=1,N
      I1=(I-1)*N+J
      1 PC(I1)=C(1,J)
      DO 2 K=1,N
      DO 2 L=1,N
      C(1,1)=A(1,K)*B(K,L)
      C(1,1)=A(1,K)*B(K,L)
      DO 3 J=1,N
      DO 3 K=1,N
      I1=(I-1)*N+J
      2 CH(I1)=PC(I1)
      RETURN
      END

```

C-----
 SUBROUTINE FORMKA(A,B,AP,B)
 DIMENSION A(4,1),B(1,4),AB(15,16)
 COMPLEX A,B,AB
 C THIS SUBROUTINE FORMS THE $(N+2) \times (N+2)$ MATRIX AB WHICH HAS THE
 C FORM $AB = A(X) \cdot B(X)$ WHERE THE CAVESES INDICATE KRONECKER PRODUCTS.
 C SEE PELLER, MATRIX ANALYSIS, OLD EDITION, P. 231.

```

      N=15
      DO 1 I=1,N
      DO 1 J=1,N
      1 AB(I,J)=CMPLX(0.,0.)
      DO 2 I=1,N
      DO 2 J=1,N
      DO 3 K=1,N
      DO 3 L=1,N
      I1=(I-1)*N+J
      I2=(I-1)*N+K
      2 AB(I1,I2)=A(1,K)*B(K,L)
      3 AB(I1,I2)=A(1,K)*B(K,L)
      RETURN
      END

```



```

100 CONTINUE
110 IF (I.EQ.1) GO TO 130, 140, 150, 160, 170, 180, 190, 200, 210, 220, 230, 240, 250, 260, 270, 280, 290, 300, 310, 320, 330, 340, 350, 360, 370, 380, 390, 400, 410, 420, 430, 440, 450, 460, 470, 480, 490, 500, 510, 520, 530, 540, 550, 560, 570, 580, 590, 600, 610, 620, 630, 640, 650, 660, 670, 680, 690, 700, 710, 720, 730, 740, 750, 760, 770, 780, 790, 800, 810, 820, 830, 840, 850, 860, 870, 880, 890, 900, 910, 920, 930, 940, 950, 960, 970, 980, 990, 1000, 1010, 1020, 1030, 1040, 1050, 1060, 1070, 1080, 1090, 1100, 1110, 1120, 1130, 1140, 1150, 1160, 1170, 1180, 1190, 1200, 1210, 1220, 1230, 1240, 1250, 1260, 1270, 1280, 1290, 1300, 1310, 1320, 1330, 1340, 1350, 1360, 1370, 1380, 1390, 1400, 1410, 1420, 1430, 1440, 1450, 1460, 1470, 1480, 1490, 1500, 1510, 1520, 1530, 1540, 1550, 1560, 1570, 1580, 1590, 1600, 1610, 1620, 1630, 1640, 1650, 1660, 1670, 1680, 1690, 1700, 1710, 1720, 1730, 1740, 1750, 1760, 1770, 1780, 1790, 1800, 1810, 1820, 1830, 1840, 1850, 1860, 1870, 1880, 1890, 1900, 1910, 1920, 1930, 1940, 1950, 1960, 1970, 1980, 1990, 2000, 2010, 2020, 2030, 2040, 2050, 2060, 2070, 2080, 2090, 2100, 2110, 2120, 2130, 2140, 2150, 2160, 2170, 2180, 2190, 2200, 2210, 2220, 2230, 2240, 2250, 2260, 2270, 2280, 2290, 2300, 2310, 2320, 2330, 2340, 2350, 2360, 2370, 2380, 2390, 2400, 2410, 2420, 2430, 2440, 2450, 2460, 2470, 2480, 2490, 2500, 2510, 2520, 2530, 2540, 2550, 2560, 2570, 2580, 2590, 2600, 2610, 2620, 2630, 2640, 2650, 2660, 2670, 2680, 2690, 2700, 2710, 2720, 2730, 2740, 2750, 2760, 2770, 2780, 2790, 2800, 2810, 2820, 2830, 2840, 2850, 2860, 2870, 2880, 2890, 2900, 2910, 2920, 2930, 2940, 2950, 2960, 2970, 2980, 2990, 3000, 3010, 3020, 3030, 3040, 3050, 3060, 3070, 3080, 3090, 3100, 3110, 3120, 3130, 3140, 3150, 3160, 3170, 3180, 3190, 3200, 3210, 3220, 3230, 3240, 3250, 3260, 3270, 3280, 3290, 3300, 3310, 3320, 3330, 3340, 3350, 3360, 3370, 3380, 3390, 3400, 3410, 3420, 3430, 3440, 3450, 3460, 3470, 3480, 3490, 3500, 3510, 3520, 3530, 3540, 3550, 3560, 3570, 3580, 3590, 3600, 3610, 3620, 3630, 3640, 3650, 3660, 3670, 3680, 3690, 3700, 3710, 3720, 3730, 3740, 3750, 3760, 3770, 3780, 3790, 3800, 3810, 3820, 3830, 3840, 3850, 3860, 3870, 3880, 3890, 3900, 3910, 3920, 3930, 3940, 3950, 3960, 3970, 3980, 3990, 4000, 4010, 4020, 4030, 4040, 4050, 4060, 4070, 4080, 4090, 4100, 4110, 4120, 4130, 4140, 4150, 4160, 4170, 4180, 4190, 4200, 4210, 4220, 4230, 4240, 4250, 4260, 4270, 4280, 4290, 4300, 4310, 4320, 4330, 4340, 4350, 4360, 4370, 4380, 4390, 4400, 4410, 4420, 4430, 4440, 4450, 4460, 4470, 4480, 4490, 4500, 4510, 4520, 4530, 4540, 4550, 4560, 4570, 4580, 4590, 4600, 4610, 4620, 4630, 4640, 4650, 4660, 4670, 4680, 4690, 4700, 4710, 4720, 4730, 4740, 4750, 4760, 4770, 4780, 4790, 4800, 4810, 4820, 4830, 4840, 4850, 4860, 4870, 4880, 4890, 4900, 4910, 4920, 4930, 4940, 4950, 4960, 4970, 4980, 4990, 5000, 5010, 5020, 5030, 5040, 5050, 5060, 5070, 5080, 5090, 5100, 5110, 5120, 5130, 5140, 5150, 5160, 5170, 5180, 5190, 5200, 5210, 5220, 5230, 5240, 5250, 5260, 5270, 5280, 5290, 5300, 5310, 5320, 5330, 5340, 5350, 5360, 5370, 5380, 5390, 5400, 5410, 5420, 5430, 5440, 5450, 5460, 5470, 5480, 5490, 5500, 5510, 5520, 5530, 5540, 5550, 5560, 5570, 5580, 5590, 5600, 5610, 5620, 5630, 5640, 5650, 5660, 5670, 5680, 5690, 5700, 5710, 5720, 5730, 5740, 5750, 5760, 5770, 5780, 5790, 5800, 5810, 5820, 5830, 5840, 5850, 5860, 5870, 5880, 5890, 5900, 5910, 5920, 5930, 5940, 5950, 5960, 5970, 5980, 5990, 6000, 6010, 6020, 6030, 6040, 6050, 6060, 6070, 6080, 6090, 6100, 6110, 6120, 6130, 6140, 6150, 6160, 6170, 6180, 6190, 6200, 6210, 6220, 6230, 6240, 6250, 6260, 6270, 6280, 6290, 6300, 6310, 6320, 6330, 6340, 6350, 6360, 6370, 6380, 6390, 6400, 6410, 6420, 6430, 6440, 6450, 6460, 6470, 6480, 6490, 6500, 6510, 6520, 6530, 6540, 6550, 6560, 6570, 6580, 6590, 6600, 6610, 6620, 6630, 6640, 6650, 6660, 6670, 6680, 6690, 6700, 6710, 6720, 6730, 6740, 6750, 6760, 6770, 6780, 6790, 6800, 6810, 6820, 6830, 6840, 6850, 6860, 6870, 6880, 6890, 6900, 6910, 6920, 6930, 6940, 6950, 6960, 6970, 6980, 6990, 7000, 7010, 7020, 7030, 7040, 7050, 70
```


REPORT DOCUMENTATION PAGE		READ INSTRUCTIONS BEFORE COMPLETING FORM
1. REPORT NUMBER	2. GOVT ACCESSION NO.	3. RECIPIENT'S CATALOG NUMBER
4. TITLE (and Subtitle) A Further Study of the Multichannel Maximum Entropy Spectral Analysis		5. TYPE OF REPORT & PERIOD COVERED Technical Report
6. AUTHOR(s) C. H. Chen and Gia-Kinn Young		7. PERFORMING ORG. REPORT NUMBER SMU-EE-TR-82-2
8. PERFORMING ORGANIZATION NAME AND ADDRESS Department of Electrical Engineering Southeastern Massachusetts University North Dartmouth, Massachusetts 02747		9. CONTRACT OR GRANT NUMBER(s) N00014-79-C-0494
10. CONTROLLING OFFICE NAME AND ADDRESS Statistics and Probability Program Office of Naval Research, Code 436 Arlington, Virginia 22217		11. PROGRAM ELEMENT, PROJECT, TASK AREA & WORK UNIT NUMBERS NR 042-422
12. MONITORING AGENCY NAME & ADDRESS (if different from Controlling Office)		13. REPORT DATE February 12, 1982
		14. NUMBER OF PAGES 41
		15. SECURITY CLASS. (of this report) Unclassified
		16. SECURITY CLASSIFICATION DOWNGRADING SCHEDULE

16. DISTRIBUTION STATEMENT (of this Report)

APPROVED FOR PUBLIC RELEASE: DISTRIBUTION UNLIMITED.

17. DISTRIBUTION STATEMENT (of the abstract entered in Block 20, if different from Report)

18. SUPPLEMENTARY NOTES

19. KEY WORDS (Continue on reverse side if necessary and identify by block number)

Maximum entropy power spectrum; multichannel spectral analysis; cross power spectrum; estimation of phase difference; coherence; eigenspectrum analysis; line-splitting and frequency shifting; computer program listing.

20. ABSTRACT (Continue on reverse side if necessary and identify by block number)

Based on the multichannel generalization of the Burg's maximum entropy spectral analysis, the report reviews the computing procedures and closely examines the software realization problem by using sinusoids as examples. The high-resolution auto- and cross spectra available are practically significant. For example, the phase difference estimate is useful for time delay estimation. The line-splitting and frequency shifting phenomena are more evident in real signals than in multichannel complex signals. Detailed

computer program listing is provided.

DD FORM 1 JAN 73 1473

EDITION OF 1 NOV 65 IS OBSOLETE

1. (10) (1) (1) (1) (1)

SECURITY CLASSIFICATION OF THIS PAGE (When Data Entered)

